

# Comparison between chiral and meson-theoretic nucleon-nucleon potentials through $(p,p')$ reactions

F. Sammarruca and D. Alonso

*Physics Department, University of Idaho, Moscow, ID 83844, U.S.A*

E.J. Stephenson

*Indiana University Cyclotron Facility, Bloomington, IN 47408 U.S.A.*

(November 4, 2018)

We use proton-nucleus reaction data at intermediate energies to test the emerging new generation of chiral nucleon-nucleon (NN) potentials. Predictions from a high quality one-boson-exchange (OBE) force are used for comparison and evaluation. Both the chiral and OBE models fit NN phase shifts accurately, and the differences between the two forces for proton-induced reactions are small. A comparison to a chiral model with a less accurate NN description sets the scale for the ability of such models to work for nuclear reactions.

21.30.Fe, 25.40.Ep, 24.10.Cn, 24.70.+s

Chiral perturbation theory ( $\chi$ PT) offers a way to describe phenomena at nuclear physics energies that is consistent with the symmetries of the underlying theory of strong interactions (QCD). In this low momentum regime, QCD itself is non-perturbative. In  $\chi$ PT, one expands chiral  $\pi N$  Lagrangians in powers of the relevant momenta or masses (*e.g.*, pion mass), relative to the QCD scale at  $\Lambda_{\text{QCD}} \sim 1$  GeV. The nucleon-nucleon (NN) force can then be derived from chiral Lagrangians by taking into account all the pion-exchange diagrams which contribute to the NN interaction at a given chiral order. NN potentials based on  $\chi$ PT are thus best suited for applications at the lowest energies. An important energy range opens near 200 MeV where the impulse approximation treatment becomes a meaningful test of the ability of an NN potential to describe nucleon-induced reactions on nuclei. Only recently has a chiral NN potential become available through the work of Entem and Machleidt (EM) [1] that accurately reproduces NN phase shifts at this energy. In this paper, we present the first tests of a chiral potential using  $(p,p')$  reactions.

Proton-nucleus elastic and inelastic scattering to selected transitions can be a “laboratory” for the evaluation of NN interactions [2–4]. Through polarization observables,  $(p,p')$  reactions are selectively sensitive to specific amplitudes in the effective interaction [5,6] constructed by placing that NN interaction in the nuclear medium. Natural-parity transitions, for example, sample the central and spin-orbit terms in the isoscalar channel. “Spin-flip” states can examine all the spin-dependent terms of either isospin. Here we will use specific  $(p,p')$  transitions from a study at 200 MeV [2,3] to compare two recent  $\chi$ PT NN potentials [1,7] with calculations based on a more conventional one-boson-exchange (OBE) potential. The two  $\chi$ PT potentials differ in the precision with which they reproduce NN phase shifts. This will calibrate for us the quality of agreement needed in  $\chi$ PT to describe reactions such as proton-nucleus elastic and inelastic scattering. Previous studies using conventional potentials demonstrated that good reproduction of  $(p,p')$  observables depends on a high quality representation of the NN data as well [2].

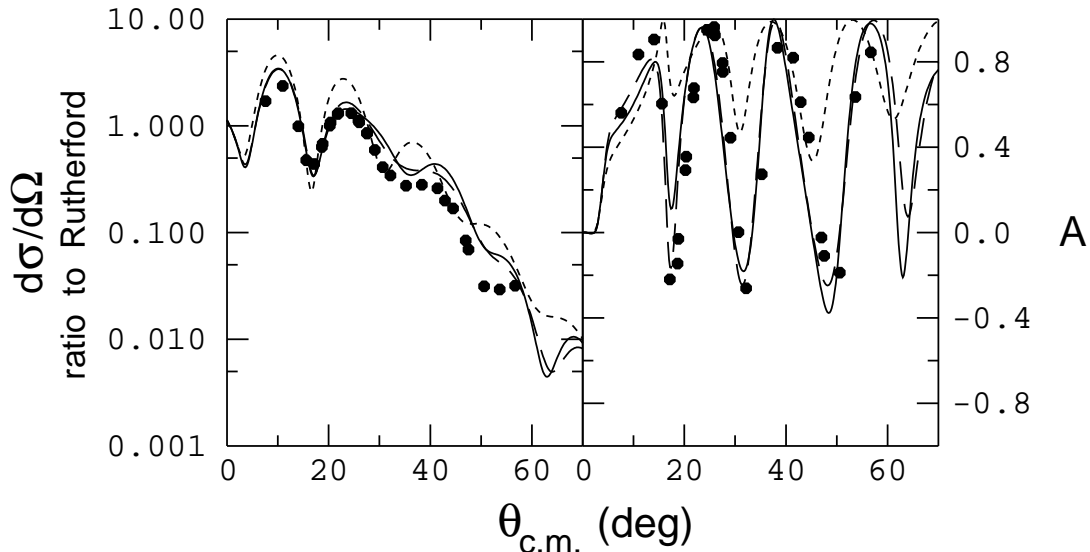


FIG. 1. Measurements for proton elastic scattering cross section (shown as the ratio to the Rutherford cross section) and analyzing power from Ref. [14]. Calculations are based on the chiral NN potential of Ref. [1] (solid curves) and the CD-Bonn potential of Ref. [9] (long-dashed curves). Both calculations contain BHF density dependence. The short-dashed curves are CD-Bonn potential calculations with no density dependence included.

The  $\chi$ PT potential of EM [1] is based on a heavy baryon expansion scheme, where nucleon fields are represented by 2-component spinors. This makes a relativistic treatment of nucleons in nuclear matter (Dirac-Brueckner-Hatree-Fock, or DBHF, approach) not feasible. Thus we will only include Brueckner-Hartree-Fock (BHF) medium effects when calculating density-dependent effective interactions.

The  $\chi$ PT expansion includes 1- $\pi$  and 2- $\pi$  diagrams from effective chiral Lagrangians, with relativistic corrections, through third order. The short-range repulsion is described by including contact terms up through fourth order. To be suitable for iteration in a Lippmann-Schwinger equation, the potential is regularized through a set of cutoff masses. The 46 model parameters were adjusted to match the NN phase shift solution from the Nijmegen group [8]. The resulting agreement is excellent at energies below 300 MeV.

The OBE model that we have chosen for comparison is the CD-Bonn potential [9]. Medium modifications arise from an effective nucleon mass (produced in a self-consistent calculation of nuclear matter saturation properties) and a spherically averaged Pauli blocking operator [10]. The resulting density-dependent G-matrix is transformed into a Yukawa representation for use in distorted wave impulse approximation (DWIA) ( $p, p'$ ) reaction calculations (see App. A of [2]).

The DWIA calculations are made with the programs LEA [11] for natural parity transitions and DWBA86 [12] for un-natural parity. The distortions are generated from the density-dependent effective interaction using the folding model. The formfactors are chosen to conform to  $(e, e')$  measurements for the same transitions. The nuclear matter density is extracted from the charge density by unfolding the formfactor of the proton [13]. Additional details may be found in Refs. [2,3].

Figures 1 and 2 show density-dependent calculations of the differential cross section

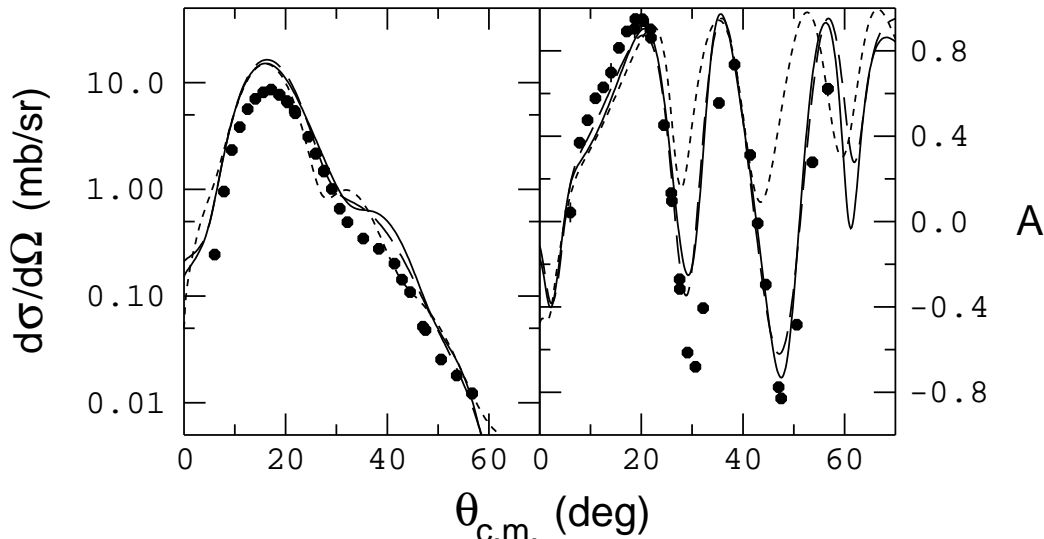


FIG. 2. Measurements for proton inelastic scattering cross section and analyzing power for the  $3^-$  state in  $^{40}\text{Ca}$  at 3.736 MeV from Ref. [14]. The curves are the same as in Fig. 1.

and vector analyzing power for 200-MeV protons incident on  $^{40}\text{Ca}$ . Figure 1 shows elastic scattering while Fig. 2 presents inelastic scattering to the  $3^-$  state at 3.736 MeV. The data are from Ref. [14]. The solid curves are based on the chiral NN potential while the long-dashed curves make use of the conventional OBE potential. The agreement between these two is good. Both calculations include the BHF medium effects described above. To demonstrate the size of these medium corrections, the short-dashed curves are free-space predictions from the CD-Bonn potential (the chiral force shows a similar change when medium effects are removed). Such a change is much larger than the differences between the chiral and OBE potentials.

Previous studies [2] have shown that a relativistic treatment of the medium improves the analyzing power for elastic scattering and inelastic scattering to natural-parity states, which is where medium effects are most clearly seen through the central and spin-orbit components of the interaction. Thus, the differences between the data and the two BHF curves may indicate problems with the treatment of the medium rather than with the basic interaction. Compared to these theoretical uncertainties, the difference between the chiral and OBE calculations is small, and we consider the chiral calculations shown here for proton-induced reactions to be very satisfactory. Since elastic scattering and the excitation of the  $3^-$  state are both natural parity transitions, this good agreement applies primarily to the central and spin-orbit components of the effective NN interaction. These are the largest parts of the isoscalar interaction.

An evaluation of the isovector part of the chiral potential is best made by a comparison to a high-spin, unnatural-parity ( $p, p'$ ) transition. A set of data that includes polarization transfer can be used to judge the correct size of each of the spin-dependent terms in the NN amplitude [5,6]. For the highest spins, the transition is reduced to a simple particle-hole excitation in which the transferred  $J$  is the sum of the individual contribution:  $J = j_{\text{part}} + j_{\text{hole}}$ . Such transitions take place in the nuclear surface where the density is small and usually show minimal effects from the density dependence of the effective interaction.

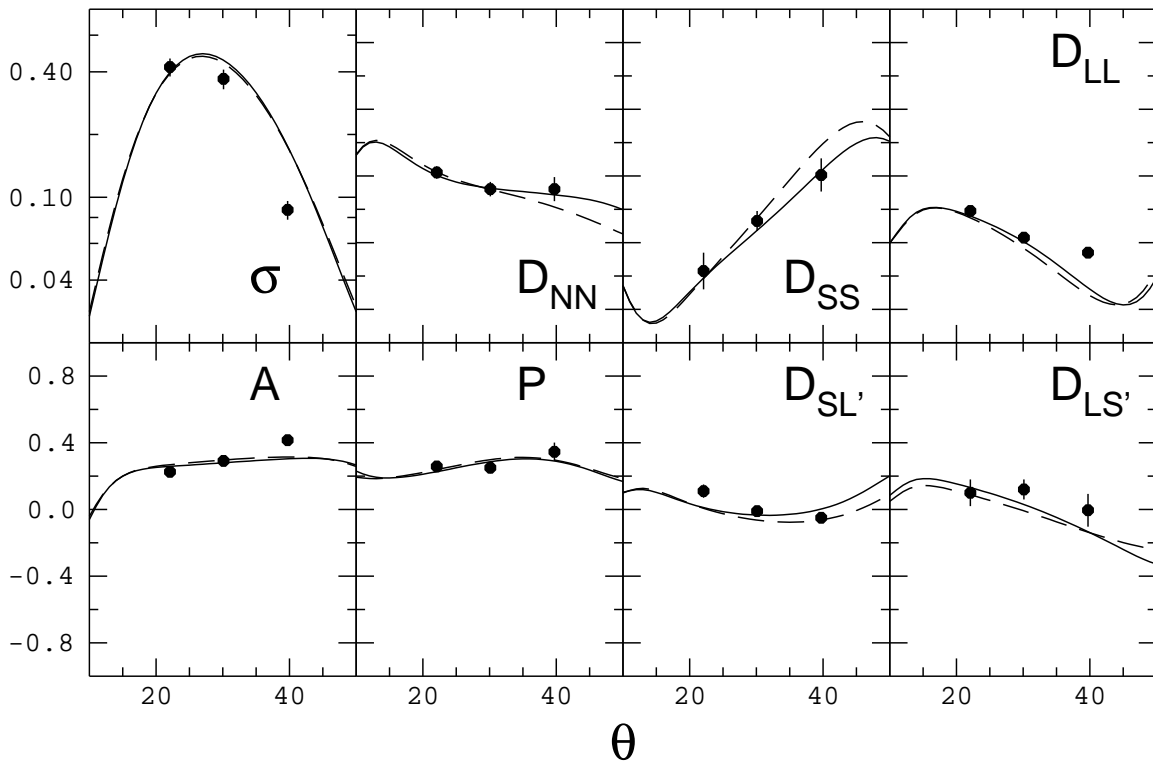


FIG. 3. Measurements of the cross section and polarization observables for the transition to the  $4^-$ ,  $T=1$  state at 18.98 MeV in  $^{16}\text{O}$  from Refs. [15,16]. The solid (dashed) curves are based on the chiral potential of Ref. [1] (the CD-Bonn potential of Ref. [9]).

Figure 3 presents the chiral and CD-Bonn calculations (solid and dashed curves, respectively) for the  $4^-$ ,  $T=1$  transition in  $^{16}\text{O}$  to the state at 18.98 MeV. BHF density dependence is included. The measurements are taken from Refs. [15,16]. The agreement between the two potentials, and with the measurements, is excellent. Interestingly, the chiral potential shows better agreement with the data for  $D_{NN}$  and  $D_{SS}$  than does the original CD-Bonn potential. This improvement comes from a small reduction in the spin-longitudinal amplitude (associated with the  $\sigma_{1q}\sigma_{2q}$  tensor operator).

In EM [1], the reproduction of the NN phase shifts up to 300 MeV was compared to the predictions from the second order [or next-to-leading order (NLO)] and the third order [or next-to-next-to-leading order (NNLO)] potentials of Ref. [7]. The second order interaction from that work has been used recently as the basis for Faddeev calculations of three-body observables [17]. Some success was found for energies near and below 10 MeV. However, at 200 MeV the phase shift predictions diverge [1]. So it is important to see at what level these differences also appear in (p,p') reactions. In Fig. 4, we again show the polarization measurements for the  $4^-$ ,  $T=1$  state in  $^{16}\text{O}$ . The solid curves are based on the EM chiral model. In this case, we are showing free-space predictions, since we are mainly interested in identifying baseline differences among the various forces. Furthermore, medium effects for this transition are small (compare the solid curves in Fig. 3 and Fig. 4), and thus would not alter the picture in a significant way. The long-dashed and short-dashed curves in Fig. 4 show the NLO and NNLO interactions of Ref. [7], respectively. The NNLO contains

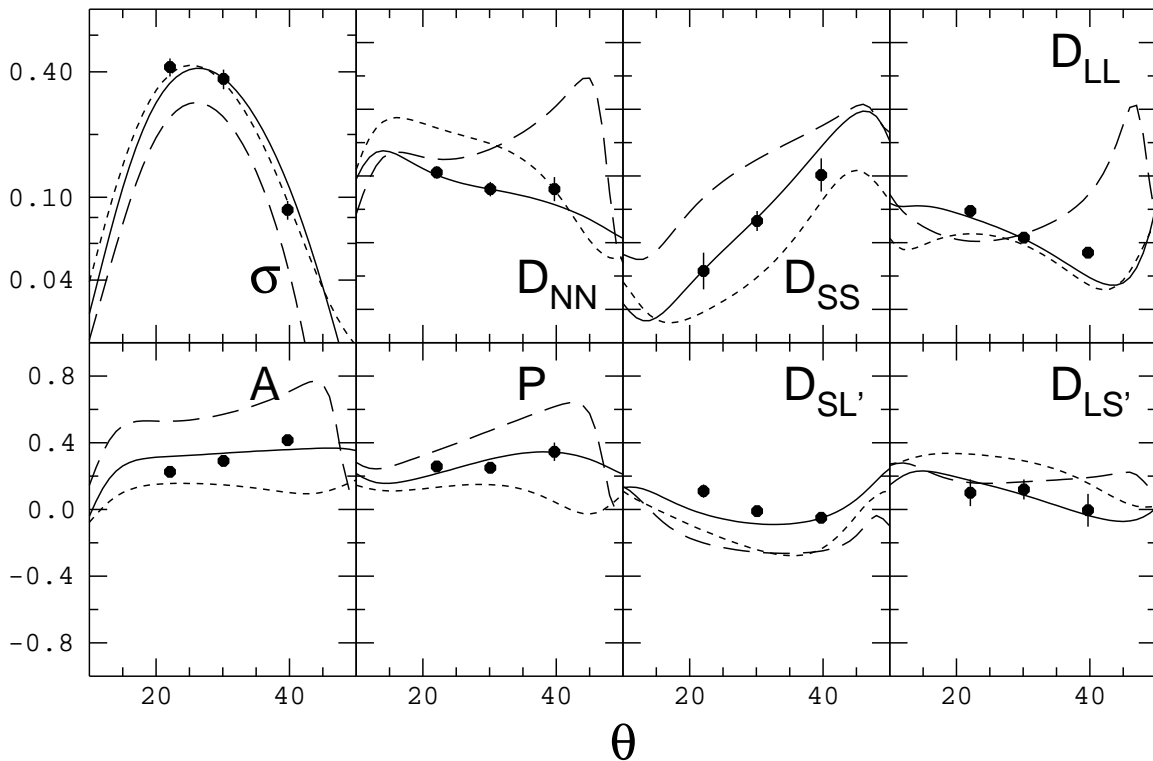


FIG. 4. The measurements are described in Fig. 3. The solid curves are based on the chiral potential of Ref. [1]. The long- and short-dashed curves are based on the NLO and NNLO potentials of Ref. [7].

pion-exchange contributions to the same order as in EM. The main difference is that EM have included contact terms to fourth order and increased the number of momentum cutoff parameters. While this increases the number of free parameters to be determined from the NN phase shifts, it also provides the flexibility necessary for an accurate fit at higher energies. The NLO and NNLO curves shown in Fig. 4 both differ dramatically from the measurements and even at NNLO do not appear to be converging. These differences exceed by an order of magnitude those shown in Fig. 3. This sets a scale for how much better the phase shift reproduction must be before it makes sense to compare these chiral potential predictions with nuclear reaction measurements at the level of conventional models. The chiral potential of EM meets this standard.

The  $\chi$ PT model of EM gives rise to a number of solutions that differ in some of their short-range characteristics. This is illustrated by excellent agreement with the long-range properties of the deuteron (binding energy, quadrupole moment, asymptotic S- and D-states, and the mean radius) while allowing the D-state probability to vary by a factor of two. These solutions provide comparable fits to NN phase shifts. Thus the handling of the short-range part via contact terms brings about a larger degree of flexibility as compared to the usual meson exchange picture (where, for instance, the strength of the tensor force as measured from the deuteron D-state probability is much more tightly constrained). Because of the restrictions imposed by the  $\chi$ PT expansion on the typical momenta involved in NN scattering or a nuclear reaction, it may not be possible to explore and control these ambiguities by going

to higher energies. Instead, we may need to examine other nuclear reactions in situations that emphasize the upper end of the allowed momentum range, such as one finds in large angle scattering or where the only contributing amplitudes come from nucleon exchange. Such an investigation is beyond the scope of this paper.

The test calculations shown here demonstrate that  $\chi$ PT models of the NN interaction can be made with sufficient accuracy to be used in calculations of nucleon-induced reactions on nuclei, at least up to 200 MeV. For this, a high precision reproduction of the NN scattering phase shifts is an essential requirement. This means that models intended for wide application must contain a sufficient amount of flexibility to make such a high precision reproduction possible. It will be the object of a future work to explore further the predictive power of high-precision potentials based on  $\chi$ PT.

### ACKNOWLEDGMENTS

The authors acknowledge financial support from the U.S. Department of Energy under grant No. DE-FG03-00ER41148 (F.S. and D.A.) and from the National Science Foundation under grant NSF-PHY-9602872 (E.S.).

- 
- [1] D.R. Entem and R. Machleidt, LANL archive preprints nucl-th/0107057 and nucl-th/0108057.
  - [2] F. Sammarruca, E.J. Stephenson, and K. Jiang, Phys. Rev. C **60**, 064610 (1999).
  - [3] F. Sammarruca, E.J. Stephenson, K. Jiang, J. Liu, C. Olmer, A.K. Opper, and S.W. Wissink, Phys. Rev. C **61**, 014309 (2000).
  - [4] F. Sammarruca and E.J. Stephenson, Phys. Rev. C **64**, 034006 (2001).
  - [5] J.M. Moss, Phys. Rev. C **26**, 727 (1982).
  - [6] E. Bleszynski, M. Bleszynski, and C.A. Whitten, Jr., Phys. Rev. C **26**, 2063 (1982).
  - [7] E. Epelbaum, W. Glöckle, and Ulf-G. Meißner, Nucl. Phys. A **637**, 107 (1998); *ibid.* **671**, 295 (2000).
  - [8] V.G.J. Stoks *et al.*, Phys. Rev. C **48**, 792 (1993).
  - [9] R. Machleidt, Phys. Rev. C **63**, 024001 (2001).
  - [10] M.I. Haftel and F. Tabakin, Nucl. Phys. **A158**, 1 (1970).
  - [11] James J. Kelly, program manual for LEA, 1995.
  - [12] R. Schaeffer and J. Raynal, program DWBA70; S. Austin, W.G. Love, J.R. Comfort, and C. Olmer, extended version DWBA86 (unpublished).
  - [13] H. de Vries, C.W. de Jager, and C de Vries, At. Data Nucl. Data Tables **36**, 495 (1987).
  - [14] H. Seifert *et al.*, Phys. Rev. C **47**, 1615 (1993).
  - [15] A.K. Opper, S.W. Wissink, A.D. Bacher, J. Lisantti, C. Olmer, R. Sawafta, E.J. Stephenson, and S.P. Wells, Phys. Rev. C **63**, 034614 (2001).
  - [16] C. Olmer, in *Antinucleon- and Nucleon-Nucleus Interactions*, edited by G.E. Walker *et al.*, (Plenum, New York, 1985), p. 261.
  - [17] E. Epelbaum, H. Kamada, A. Nogga, H. Witała, W. Glöckle, and Ulf-G. Meißner, Phys. Rev. Lett. **86**, 4787 (2001).